Evaluation of Textural Feature Extraction Methods for Prostate Cancer TRUS Medical images

R. Manavalan

Department of Computer Science (PG)
K.S.R College of Arts and Science
Thiruchengode, Tamilnadu, India

K. Thangavel

Department of Computer Science
Periyar University, Salem – 636 011.
Tamilnadu, India.

ABSTRACT

Ultrasound imaging is one of the promising techniques used for early detection of prostate cancer. The image is segmented by different methods after preprocessing. In this paper, DBSCAN clustering with morphological operators is used to extort the prostate region. It is proposed to analyze the performance of the features extracted from the different Gray Level Co-occurrence Matrix (GLCM) constructed for various distances with different combination of directions, since there is no research has been conducted so far. Then, Support Vector Machine (SVM) is used to classify the images into benign or malignant using the extracted features. The performance of the classification is evaluated using various statistical measures such as sensitivity, specificity and accuracy. The proposed method is tested over 5500 digitized TRUS images of prostate.

Keywords

Support Vector Machine; SVM; Gray Level Co-occurrence Matrix; GLCM; DBSCAN; M3-Filter.

1. INTRODUCTION

Digital image plays a vital role in the early detection of cancers, such as prostate cancer, breast cancer, lungs cancer, cervical cancer and blood cancer. Prostate cancer is now most frequently diagnosed male malignancy with one in every 11 men [19]. It is the second position in cancer–related cause of death only for male population [16]. Ultrasound imaging method is suitable to diagnosis and prognosis. An accurate detection of region of interest in ultrasound image is crucial, since the result of reflection, refraction and deflection of ultrasound waves from different types of tissues with different acoustic impedance. Usually, the contrast in ultrasound image is very low and boundary between region of interest and background are more uncertain [15]. Images are prone to different types of noises. Noise is considered to be any measurement that is not part of the phenomena of interest. And also speckle noise and weak edges make the image difficult to identify the prostate region in the ultrasound image. So, the analysis of ultrasound image is more challenging one. Generally there are two common use of ultrasound medical imaging: first one is to guide the oncologist in the biopsy procedure and second is in the establishing the volume of the prostate. It has been used in diagnosing for more than 50 years. The statistical textural features can be extracted from the segmented region to classify the proteomic into benign or malign. This paper emphasis textural features extraction from GLCM for various distances and directions. Support Vector

Machine (SVM) is adopted for classification. The following section presents an overview of the proposed system.

1.1. Overview of the System

The proposed system consists of five stages such as acquisition of TRUS image of prostate, preprocessing, segmentation, feature extraction and classification. The overview of the proposed system is depicted in fig 1. Computer Aided Diagnosis (CAD) system is developed for automatic detection of prostate tumor in Transrectal Ultrasound (TRUS) image. It can provide the valuable viewpoint and accuracy of earlier prostate cancer detection.
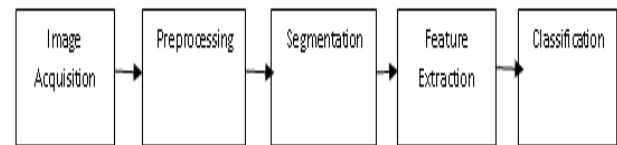

Fig 1: CAD System

The detailed description of each stage is presented in the subsequent sections. The rest of the paper is organized as follows: section 2 deals about Image Acquisition and preprocessing of original TRUS medical image of prostate. The DBSACN clustering with morphological operators for locating the Region of Interest (ROI) from TRUS prostate medical image is described in section 3. The feature extraction through GLCM is illustrated in section 4. The SVM classifier is discussed in section 5. The experimental analysis and discussion are presented in the section 6. Section 7 concludes this work with further directions.

2. IMAGE ACQUITIONS AND PREPROCESSING

Ultrasound imaging is a widely used technology for prostate cancer diagnosis and prognosis among the different medical image modalities. Image acquisition processes required less than 30 minutes for each case. The TRUS images of the prostate gland were acquired while the TRUS probe was supported and manipulated by the TRUS Robot using a joystick located next to the console, without the need for a dedicated assistant. The entire prostate was scanned by rotating the TRUS probe about its axis, minimizing prostate displacement and deformation. The probe depth can be manually adjusted by a surgeon. Accurate recording of images and corresponding TRUS frame coordinates were obtained. The gathered information was used in offline

segmentation for the ultrasound image of the prostate gland. Image acquisition is done from ultrasound device via frame grabber. Image of the prostate can be generated using a series of TRUS images. The ultrasound images are very difficult to segment because of poor image contrast, speckle noise, and missing or diffuse boundaries in the transrectal ultrasound (TRUS). M3-Filter is used to generate a despeckled image since the speckle noise is commonly found in the ultrasound medical images [15]. The common form of noise is data dropout noise generally referred to as speckle noise [18]. This noise is, in fact, caused by errors in data transmission. The corrupted pixels are either set to the maximum value, which is something like a snow in image or have single bits flipped over. This kind of noise affects the ultrasound images. Hence, the information of edges is needed for the proper segmentation. Once the noise is removed to enhance the contrast of the image, the imtophat filter has been used to create with required edges. The enhanced image is segmented using DBSCAN clustering discussed in the following section.

3. IMAGE SEGMENTATION

Local adaptive thresholding method used to simplify the image segmentation process to change the enhanced grayscale image into a binary image, in which each pixel is restricted to a value of either 0 or 1. The techniques used on these binary images go by morphological operators Opening and Closing [2] [9]. The area must be isolated from other white regions in the thresholded image is a difficult task in TRUS prostate medical images. The thresholded image can be reconstructed by using Opening and Closing operators with a large disk structuring element to isolate the object with high likelihood to be part of the prostate can be distinguished [9]. With the aim of separating background from TRUS image to target possible prostate, pixels of thresholded images are grouped by using DBSCAN [7] [17]. It takes a binary (segmented) image, and delineates only significantly important regions by clustering. The expected outcome is desired boundary of the TRUS prostate image. A sample image and its segmented image are provided in fig 2(a) and fig 2(b) respectively. The DBSCAN Algorithm for segmentation is detailed in fig 3.

Once the two parameters eps and minPts are fixed, DBSCAN starts to cluster data points from an arbitrary point q. It begins by finding the neighborhood of point q, that is all points that are directly density reachable from the point q. For an image, we start with left-top pixel (not necessarily a corner pixel, any arbitrary pixel can be chosen for first iteration) as our first point in the sub image. We look for first pixel satisfying the core pixel condition as a starting (seed) point.
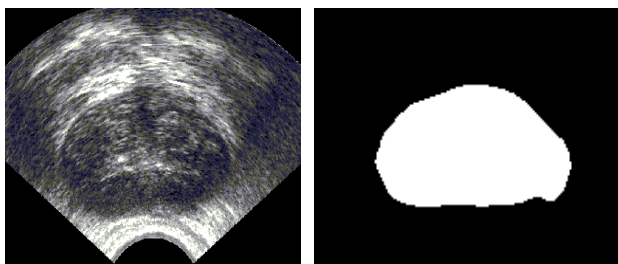

Fig 2(a) - original image   **2(b) – segmented image**

DBSCAN Algorithm
INPUT: Enhanced TRUS prostate image
OUTPUT: Segmented image which contains only prostate

Step1: Set epsilon (eps) and minimum points (minPts).

Step2: Starts with an arbitrary starting point that has not been visited and then finds all the neighbor points within distance eps of the starting point.

Step3: If the number of neighbors is greater than or equal to minPts, a cluster is formed. The starting point and its neighbors are added to this cluster and the starting point is marked as visited. The algorithm then repeats the evaluation process for all the neighbors recursively.

Step4: If the number of neighbors is less than minPts, the point is marked as noise.

Fig 3: DBSCAN Algorithm

If the neighborhood is sparsely populated, i.e. it has fewer than MinPts points, and then the point q is labeled as noise. Otherwise, a cluster is initiated and all points in neighborhood of the point q are marked by new cluster. Next the neighborhoods of the neighborhood q are examined iteratively to check if they can be added into the cluster. If a cluster cannot be expanded further, DBSCAN chooses another arbitrary unlabeled point and repeats the process to form another cluster [12]. This procedure is iterated until all pixels in the image have been identified as noise or with a cluster of prostate pixels.

4. FEATURE EXTRACTIONS

Normally texture analysis can be grouped into four categories: model-based, statistical-based, structural-based, and transform-based methods. Structural approaches seek to understand the hierarchal structure of the image, while statistical methods describe the image using pure numerical analysis of pixel intensity values [14]. Transform approaches generally perform some kind of modification to the image, obtaining a new "response" image that is then analyzed as a representative proxy for the original image. Model-based methods are based on the concept of predicting pixel values based on a mathematical model. Texture is one of the important characteristics used in identifying an object in an image and also discriminate the images [1]. The texture coarseness or fineness of an image can be interpreted as the distribution of the elements in the matrix [10] [11]. In this paper, segmented image (ROI) is utilized to construct GLCM using the combination of various distances and directions, and then twenty two features are extracted from each GLCM for the classification of TRUS prostate image.

4.1. Gray Level Co-occurrence Matrices (GLCM)

Statistical methods use second order statistics to model the relationships between pixels within the region by constructing Gray Level Co-occurrence Matrices [11]. The GLCM is based on an estimation of the second-order joint conditional probability density functions $p(i, j \mid d, \theta)$ for various directions θ = 0, 45, 90, 135°, etc., and different distances, d= 1, 2, 3, 4 ,and 5. The function $p(i, j \mid d, \theta)$ is the probability that two pixels, which are located with an intersample distance d and a direction θ, have a gray level and a gray level i and j. The spatial relationship is defined in terms of distance d and angle θ [3]. If

the texture is coarse, and distance d is small, the pairs of pixels at distance d should have similar gray values. Conversely, for a fine texture, the pairs of pixels at distance d should often be quite different, so that the values in the GLCM should be spread out relatively uniformly [4]. Similarly, if the texture is coarser in one direction than another, then the degree of spread of the values about the main diagonal in the GLCM should vary with the direction θ. The next section explicates SVM classifier for the classification of extracted features.

5. SVM CLASSIFIER

Support vector machine is based on statistical learning technique which is well-founded in modern statistical learning theory. The Support Vector Machines were introduced by Vladimir Vapnik and his colleagues. The earliest mention was in (Vapnik, 1979). SVM is a useful technique for data classification. It is also be a leading method for solving non-linear problem. A classification task usually involves with training and testing data which consist of some data instances. Each instance in the training set contains one target values and several attributes. The goal of SVM is to produce a model which predicts target value of data instances in the testing set which are given only the attributes. Classification in SVM is an example of Supervised Learning. Known labels help indicate whether the system is performing in a right way or not. This information points to a desired response, validating the accuracy of the system, or be used to help the system learn to act correctly. A step in SVM classification involves identification as which are intimately connected to the known classes [5].

Support vector machines use the training data to crate the optimal separating hyperplane between the classes. The optimal hyperplane maximizes the margin of the closest data points. A good separation is achieved by the hyperplane that has the largest distance to the nearest training features of any class (so-called functional margin). Maximum-margin hyperplane and margins for a SVM trained with samples from two classes. Samples on the margin are called the support vectors [8]. SVM divides the given data into decision surface. Decision surface divides the data into two classes like a hyper plane. Training points are the supporting vector which defines the hyper plane. The basic theme of SVM is to maximize the margins between two classes of the hyper plane [6].

Basically, SVMs can only solve binary classification problems. They have then been extended to handle multi-class problems. The idea is to decompose the problem into many binary-class problems and then combine them to obtain the prediction. To allow for multi-class classification, SVM uses the one-against-one technique θ by fitting all binary sub classifiers and finding the correct class by a voting mechanism. The "one-against-one" approach is implemented in SVM for multiclass classification. If K is the number of classes, then K(K - 1)/2 binary classifiers are constructed and trained to separate each pair of classes against each other, and uses a majority voting scheme (max-win strategy) to determine the output prediction. For training data from the i th and the j th classes, we solve the following two-class classification problem [13]. Let us denote the function associated with the SVM model of $\{c_{i,}c_{j}\}$ as:

$$g(x)_{ij} = sign(f(x)_{ij})$$

An unseen example, x, is then classified as:

$$f(x) = \arg\max_{i} \sum_{i=1}^{K} \sum_{j=1 \wedge i \neq j}^{K} V_{ij}(x)$$

where:

$$V_{i,j}(x) = \begin{cases} 1\, if & g_{ij}(x) = 1 \\ 0\, if & g_{ij}(x) = -1 \end{cases}$$

Each feature set is examined using the Support Vector Machine classifier. In classification, we use a voting strategy: each binary classification is considered to be a voting where votes can be cast for all data points x in the end point is designated to be in a class with the maximum number of votes. In case that two classes have identical votes, though it may not be a good strategy, now we simply choose the class appearing first in the array of storing class names. The objective of any machine capable of learning is to achieve good generalization performance, given a finite amount of training data, by striking a balance between the goodness of fit attained on a given training dataset and the ability of the machine to achieve error-free recognition on other datasets. With this concept as the basis, support vector machines have proved to achieve good generalization performance with no prior knowledge of the data. The optimal separating hyperplane can be determined without any computations in the higher dimensional feature space by using kernel functions in the input space. Commonly used kernels include:

(i) Linear Kernel: $K(x, y) = x.y$

(ii) Radial Basis Function

(Gaussian) Kernel: $K(x,y) = e^{(-\|x\,-\,y\|^2/2\sigma^2)}$

(iii) Polynomial Kernel: $K(x, y) = (x.y + 1)^{d}$

6. EXPERIMENTAL ANALYSIS AND DISCUSSION

The proposed method has been implemented using MATLAB. In order to evaluate this work, experiments conducted over 5500 image with normal and abnormal cases. The total of 5500 TRUS medical images of prostate measuring 250x250 pixels is transformed into a Grey Level Co-Occurrence Matrix (GLCM) along the directions of (0º, 45º, 90º, 135º, 180 º, 225 º, 270 º, 315 º,{ 0º, 180 º},{45º, 225 º},{90º, 270 º},{135º, 315 º},{0º, 45º, 90º, 135º},{ 180 º, 225 º, 270 º, 315 º}) and five distances (1, 2, 3, 4 and 5 pixels) producing 70 Co-occurrence Matrices. From each GLCM, 22 texture features are extracted. Extracted features are fed into SVM for construct the prediction model. Then it is tested by using 550 TRUS prostate images. The performance of the prediction was evaluated in terms of sensitivity, specificity, accuracy, the respective formula are given in Table 2.

Table 2.Formula for Measures

Measures	Formula
Sensitivity	TP/(TP+FN)
Specificity	TN/(TN+FP)
Accuracy	(TP+TN)/(TP+FP+TN+FN)

Accuracy measures the quality of the classification. It takes into account true and false positives and negatives. Accuracy is generally regarded with balanced measure whereas sensitivity deals with only positive cases and specificity deals with only negative cases. TP is number of true positives, FP is number of false positives, TN is number of true negatives and FN is number of false negatives. A confusion matrix provides information about actual and predicted cases produced by classification system.

Table 3.Confusion Matrix

Actual	Predicted	
	Positive	Negative
Positive	TP	FP
Negative	FN	TN

TP-predicts cancer as cancer.
FP-predicts cancer as normal.
TN-predicts normal as normal.
FN- predicts normal as cancer.

The performance of the system is examined by demonstrating correct and incorrect patterns. They are defined as confusion matrix in Table 3. The higher value of both sensitivity and specificity shows better performance of the system. Computational results for each feature set have been presented in the Table 4. And the visual representation of the commutated results is depicted in fig 3(a) – 3(c).
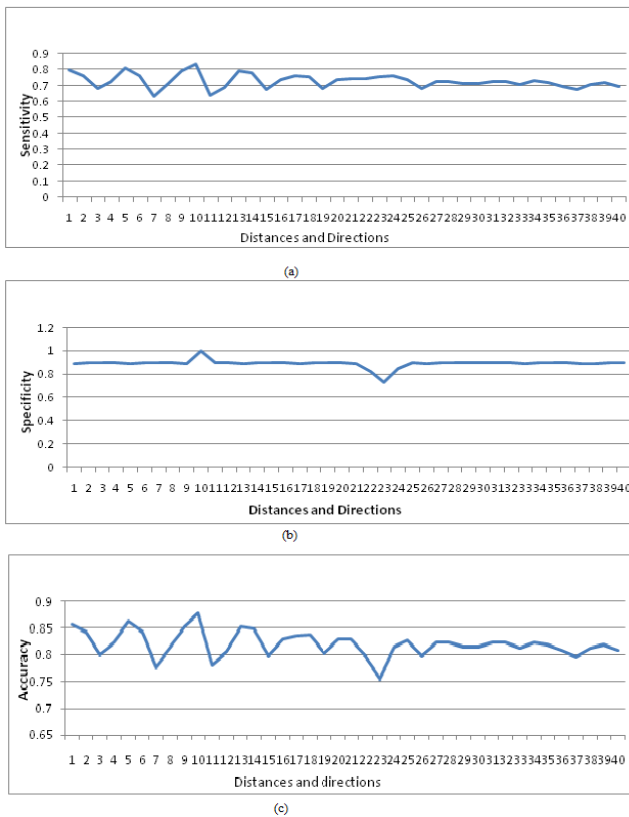

(a)

(b)

(c)

Fig 3(a)-(c) : Performance Analysis Chart for a distance and a direction

Table 5: Results of statistical parameters for a distance and symmetric pair of direction

Distance	Direction	sensitivity	Specificity	Accuracy
1	dir04	0.740749	0.896979	0.828864
	dir15	0.727991	0.9	0.823995
	dir26	0.706474	0.9	0.813237
	dir37	0.685952	0.9	0.802976
2	dir04	0.735567	0.89697	0.826268
	dir15	0.764025	0.91	0.842013
	dir26	0.721039	0.9	0.82052
	dir37	0.738572	0.9	0.829286
3	dir04	0.740749	0.896979	0.828864
	dir15	0.723476	0.9	0.821738
	dir26	0.690993	0.9	0.805497
	dir37	0.680969	0.9	0.800484
4	dir04	0.740749	0.896979	0.828864
	dir15	0.743428	0.895951	0.82969
	dir26	0.731943	0.89594	0.823942
	dir37	0.704442	0.895913	0.810177
5	dir04	0.63084	0.803226	0.727033
	dir15	0.727991	0.9	0.823995
	dir26	0.738572	0.9	0.829286
	dir37	0.73942	0.9	0.82971

Table 4: results of statistical parameters for a distance and a direction

Distance	Direction	sensitivity	Specificity	Accuracy
1	0	0.802692	0.893952	0.858322
	45	0.762857	0.900000	0.841429
	90	0.681475	0.897908	0.799692
	135	0.724701	0.900000	0.82235
	180	0.811748	0.893964	0.862856
	225	0.762857	0.900000	0.841429
	270	0.631538	0.897872	0.774705
	315	0.710336	0.900000	0.815168
2	0	0.79381	0.893939	0.853874
	45	0.837909	1.000000	0.878955
	90	0.639231	0.900000	0.779615
	135	0.689672	0.900000	0.804836
	180	0.79381	0.893939	0.853874
	225	0.779091	0.900000	0.849545
	270	0.676452	0.900000	0.798226
	315	0.739565	0.900000	0.829783
3	0	0.759908	0.893890	0.836899
	45	0.754956	0.900000	0.837478
	90	0.683008	0.900000	0.801504
	135	0.739565	0.900000	0.829783
	180	0.743874	0.893865	0.828869
	225	0.747193	0.827549	0.797371
	270	0.754956	0.733422	0.754189

Distance	Direction			
	315	0.762857	0.847576	0.815216
	0	0.737257	0.895893	0.826575
	45	0.679917	0.895825	0.797871
	90	0.724701	0.900000	0.82235
	135	0.724701	0.900000	0.82235
	180	0.714828	0.895868	0.815348
	225	0.714828	0.895868	0.815348
	270	0.724701	0.900000	0.82235
4	315	0.724701	0.900000	0.82235
	0	0.707607	0.895859	0.811733
	45	0.729649	0.895885	0.822767
	90	0.717458	0.900000	0.818729
	135	0.696446	0.900000	0.808223
	180	0.673279	0.895816	0.794547
	225	0.707607	0.895859	0.811733
	270	0.717458	0.900000	0.818729
5	315	0.696446	0.900000	0.808223

Fig 4(a) – (c): performance analysis chart for a distance and symmetric pair of direction.

Among the results obtained for various distances and directions, the table 7 and the fig 7 and fig 8 obviously quantifies that the features extracted from the GLCM for distance =2 with direction = 45 is the best classification for prostate cancer images for distinguishing malignant and benign since the value of sensitivity, specificity and accuracy are higher when compare to others.

Table 6: Results of statistical parameters for a distance and four directions.

Distance	Direction	sensitivity	Specificity	Accuracy
1	0,45,90,135	0.692273	0.9	0.806136
	180,-45,-90,-135	0.764528	0.895951	0.84024
2	0,45,90,135	0.793705	0.9	0.856853
	180,-45,-90,-135	0.747407	0.895935	0.831671
3	0,45,90,135	0.697143	0.9	0.808571
	180,-45,-90,-135	0.715	0.895902	0.815451
4	0,45,90,135	0.677989	0.9	0.798994
	180,-45,-90,-135	0.705497	0.897257	0.811377
5	0,45,90,135	0.750811	0.9	0.835405
	180,-45,-90,-135	0.738768	0.897218	0.827993

From the computational results we can notice that the features extracted from GLCM for distance = 2 with direction = 45 give very aggressive results among four quantitative performance measures with higher sensitivity and specificity rate. In order to quantify the influence of the direction choices (combination of directions), the GLCM is constructed with direction choices and distance for feature extraction. The results of performance measures are tabulated in table 5 and table 6. The fig 4(a) - (c) shows graphical representation each performance measures for a distance and symmetric pair of direction. From the table 5, it is pragmatic that the feature extracted from GLCM for distance = 2 with the symmetric directions (0 and 180) give superior results compare to others.

Similarly the table 6 and the fig 5(a) – 5(c) insists that the feature extracted from GLCM for distance d=2 with the combined directions (0, 45, 90, and 135) afford good results.

The fig 3(a-d), 4 (a-d), 5(a-d) show the performance measures of individual case for the classification over the 5500 images. The fig 6 clearly shows that absolute performance measurers chart.
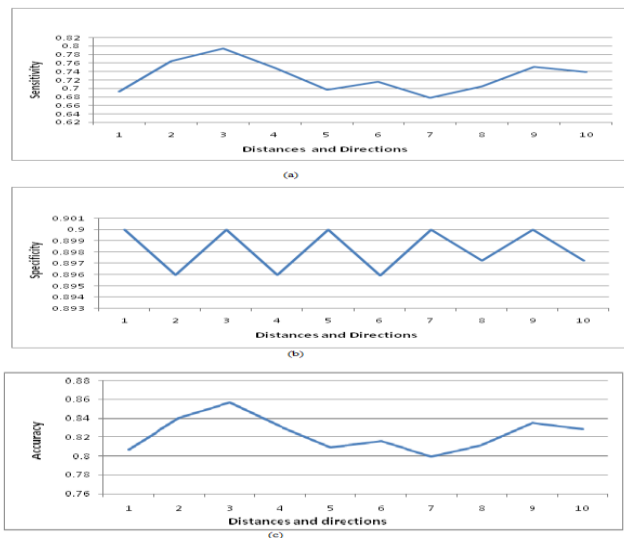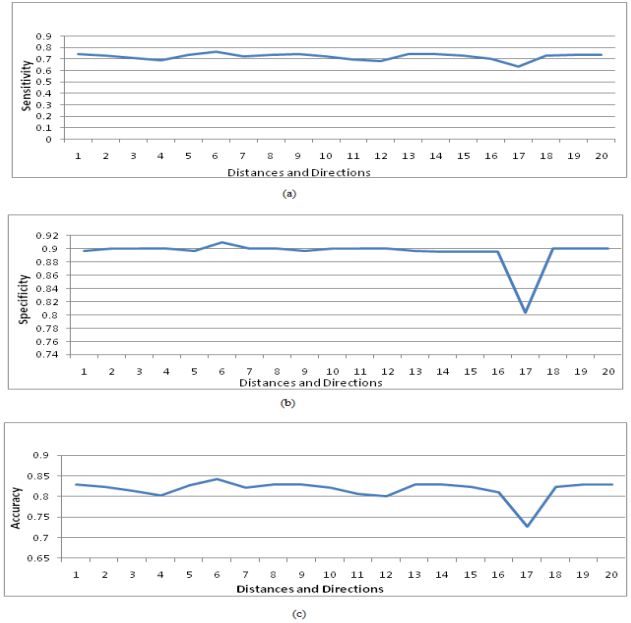

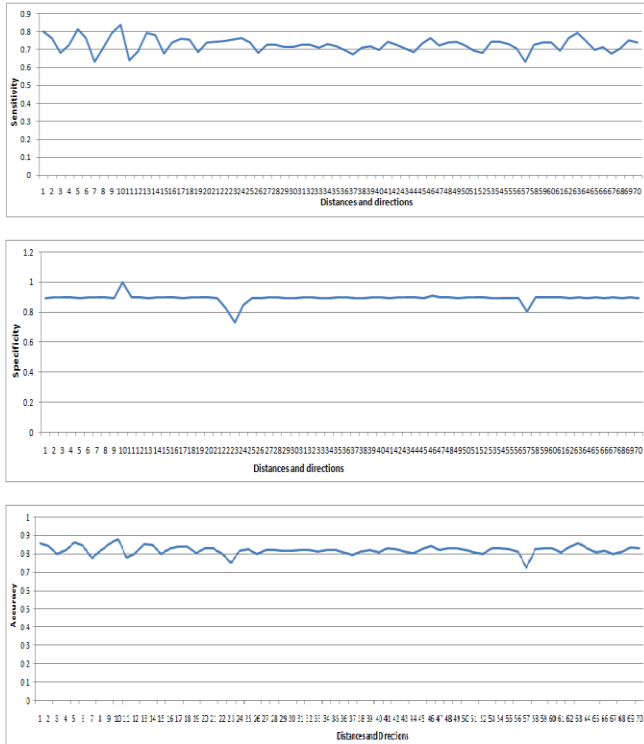**Fig 5(a) – (c): performance chart for a distance and four direction**

Fig 6: performance analysis chart for various distances and directions

Table 7: Results of statistical parameters for a distance and four directions

Distance	Direction	sensitivity	Specificity	Accuracy
2	dir26	0.764025	0.9	0.842013
2	0,45,90,135	0.793705	0.91	0.856853
2	45	0.837909	1	0.878955

The obtained results demonstrate excellent classification with 84 % sensitivity, 100% specificity and 87.89% accuracy.
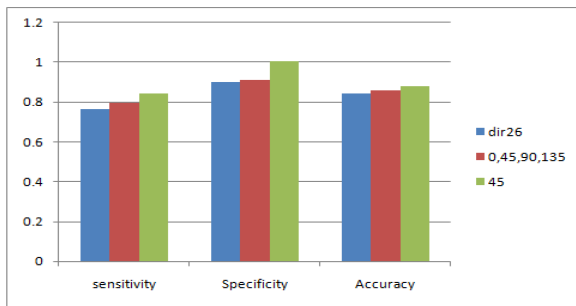

Fig 7: performance analysis chart for various distances and directions

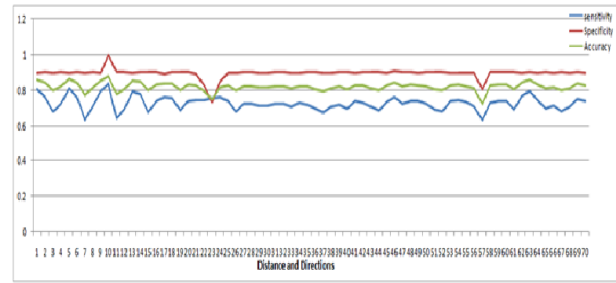The overall classification accuracy for normal is 100% and for cancer is 88%.

Fig 8: performance analysis chart

Among the classification results obtained for various distances and directions, the table 7 quantifies that the feature extracted from the GLCM for the distance =2 with direction = 45 obtained better classification results with 84 % sensitivity, 100% specificity and 87.89% accuracy where the feature extracted from the GLCM for the distance =2 with symmetric directions = {45, 225} and the distance =2 with direction = {0º, 45º, 90º, 135º } provide the least classification accuracy with 76 % sensitivity, 90% specificity and 84% accuracy and 79 % sensitivity, 91% specificity and 91% accuracy respectively.

7. CONCLUSION

TRUS imaging is one of the best methods in prostate cancer detection, but in some cases radiologists face difficulty in directing the tumors. The method presented in this paper could assist the medical staff and improve the accuracy of detection. The proposed approach effectively addresses the feature extraction problem TRUS image analysis of prostate and can also be applied to other image analysis applications. This method of feature extraction from GLCM with various distances and directions are compared and analyzed. The performance of the texture is measured using quantitative performance measures. The Performance of proposed method is tested with ultrasound image regard to prostate. The computational result showed that Texture features based on GLCM for d = 2 with θ = 45 distinguish between malignant and benign on TRUS images, with accuracy levels higher than texture features based on others. This work investigated a classification of prostate medical images using GLCM features for various distances and directions. The maximum accuracy rate for normal and cancer classification is 88%. GLCM features may be combined with other statistical features to improve the results in classification of TRUS prostate images. Using proper feature selection method accuracy may be improved efficiently in future.

8. REFERENCES

[1] Amadasun, M.   and King, R., (1989) 'Textural features corresponding to textural   properties', IEEE Transactions on Systems, Man, and Cybernetics, vol. 19, no. 5, pp. 1264 - 1274.

[2] Anil K. Jain. (1989) Fundamentals of Digital Image Processing: Prentice Hall.

[3] Babaghorbani, P.; Parvaneh, S.; Ghassemi, A.R.; Manshai, K: (2010) 'Sonography Images for Breast Cancer Texture classification in Diagnosis of Malignant or Benign Tumors', in 4th International Conference on Bioinformatics and Biomedical Engineering (iCBBE), pp.18 - 20.

[4] Chung-Ming W.; Yung-Chang C. and Hsieh, K; (1992) 'Texture features for classification of ultrasonic liver images'. Medical Imaging, IEEE Transactions on, Volume: 11 Issue: 2, pp 141 –152.

[5] Devendran V et. al.,(2008) 'Texture based Scene Categorization using Artificial Neural Networks and Support Vector Machines: A Comparative Study,' ICGST-GVIP, Vol. 8, Issue IV, pp. 45-52.

[6] Duda, R., Hart, P. And Stork, D. (2001), 'Pattern Classification': John Wiley and Sons.

[7] Ester, M., Kriegel, H.P., Sander, J., and Xu, X.(1996) 'A density-based algorithm for discovering clusters in large spatial databases with noise'. Proceedings of 2nd International Conference on Knowledge Discovery and Data Mining, Portland: AAAI Press. pp. 226-231.

[8] Fatima Eddaoudi, and Fakhita Regragui,:(2011) 'Masses Detection Using SVM Classifier Based on Textures Analysis' Applied Mathematical Sciences, Vol. 5, No. 8, pp. 367 – 379.

[9] Gonzalez, R. and Woods, R. (2002). Digital Image Processing. 3rd Edn., Prentice Hall Publications, pp. 50-51.

[10] Haralick, R.M. , Shanmugan, K.. and Dinstein, I.(1973) 'Textural Features for Image Classification', IEEE Tr. on Systems, Man, and Cybernetics, Vol SMC-3, No. 6, pp. 610-621.

[11] Haralick, R.M. (1979) 'Statistical and Structural Approaches to Texture', Proceedings of the IEEE, Vol. 67, No. 5, pp. 786-804.

[12] Massimiliano Pavan and Marcello Pelillo: (2007) 'Dominant Sets and Pairwise Clustering', IEEE Transactions On Pattern Analysis and Machine Intelligence, Vol. 29, No. 1, pp. 167 – 172.

[13] Metehan Makinacı:(2005) ' Support Vector Machine Approach for Classification of Cancerous Prostate Regions', World Academy of Science, Engineering and Technology. pp. 166 – 169.

[14] Mohamed, S.S. and Salama M.M. (2005) 'Computer Aided diagnosis for Prostate cancer using Support Vector Machine' Publication: Proc., medical imaging conference, California, SPIE Vol. 5744, pp. 899-907.

[15] Thangavel, K., Manavalan, R. and Laurence Aroquiaraj . I. (2009), Removal of Speckle Noise from Ultrasound Medical Image based on Special Filters: Comparative Study, ICGST-GVIP Journal, ISSN 1687-398X, Volume (9), Issue (III), pp. 25-32.

[16] Scardino, PT.,(1989) 'Early detection of prostate cancer'. ; Urol Clin North Am., Vol. No 16(4) , pp: 635-55.

[17] Sinan Kockara, Mutlu Mete, Bernard Chen, and Kemal Aydin:(2010). 'Analysis of density based and fuzzy c-means clustering methods on lesion border extraction in dermoscopy images', From Seventh Annual MCBIOS Conference: Bioinformatics Systems, Biology, Informatics and Computation Jonesboro, AR, USA. pp. 19 - 20.

[18] Sinha, G.R., Kavita Thakur and Kowar, M.K. (2008). "Speckle reduction in Ultrasound Image processing", Journal of Acoustical. Society of India, Vol. 35, No. 1, pp. 36-39.

[19] Yanong Zhu, Stuart Williams, and Reyer Zwiggelaar (2006), 'Computer Technology in Detection and Staging of Prostate Carcinoma: A review, Medical image Analysis' Vol. No.10, pp 178-199